

# Interference Cancellation Architecture for Full-Duplex System with GFDM Signaling

Wonsuk Chung and Daesik Hong

School of Electrical and Electronic Eng., Yonsei University  
Yonsei-ro, Seodaemun-gu, Seoul, Korea, 120-749  
Email: {wsk1111, daesikh}@yonsei.ac.kr

Risto Wichman and Taneli Riihonen

School of Electrical Engineering, Aalto University  
P.O. Box 13000, FI-00076 Aalto, Finland  
Email: {risto.wichman, taneli.riihonen}@aalto.fi

**Abstract**—This paper concerns the design of in-band full-duplex transceivers that employ generalized frequency-division multiplexing (GFDM). The composite of these two timely concepts is a promising candidate technology for emerging 5G systems since the GFDM waveform is advantageous to flexible spectrum use whereas full-duplex operation can significantly improve spectral efficiency. The main technical challenge in full-duplex transceivers at large is to mitigate their inherent self-interference due to simultaneous transmission and reception. In the case of GFDM that is non-orthogonal by design, interference cancellation becomes even more challenging since the interfering signal is subject to intricate coupling between all subchannels. Thus, we first develop a sophisticated frequency-domain cancellation architecture for removing all the self-interference components. Furthermore, by exploiting the specific structure of the interference pattern, we further modify the scheme into one that allows flexible control and reduction of computational complexity. Finally, our simulation results illustrate the trade-off between cancellation performance and system complexity, giving insights into the implementation of interference cancellation when we aim at achieving both low error rate and low complexity.

## I. INTRODUCTION

One of the core transmission techniques in current modern wireless systems is indisputably orthogonal frequency-division multiplexing (OFDM) which modulates transmitted data on inter-carrier interference-free subchannels in order to offer high spectral efficiency with simple implementation. However, the OFDM modulation has reached its limits for supporting highly increasing data rates and diversifying applications due to the inflexibility of the orthogonal format [1], and recent rapid developments already focus on envisioning and establishing several kinds of new advanced data transmission techniques [2] for replacing OFDM. Especially, filter-bank multi-carrier modulation (FBMC) has recently been highlighted as a viable alternative to OFDM in fifth-generation (5G) mobile communication systems [1].

As an apt example of FBMC-based transmission, *generalized frequency-division multiplexing* (GFDM) considered herein is a potential modulation technique [3] whose pulse-shaping filter can be designed to have desired properties, e.g., low out-of-band (OOB) radiation, for facilitating spectrum flexibility [3], [4]. Likewise, the cyclic prefix (CP) of GFDM

solves problems related to synchronization and robustness to multipath propagation [5]. As we expect that GFDM makes up for the weaknesses of its orthogonal ancestors, it is now under investigation in various kinds of 5G scenarios such as machine-type communication and cognitive radios [4], [6].

This paper investigates the design of GFDM transceivers in conjunction with in-band full-duplex technology that is one of the key 5G concepts and targets at doubling spectral efficiency [7], [8]. First and foremost, a full-duplex transceiver has to cope with self-interference (SI), namely that the transmitted signal loops back to the transceiver and is mixed with signal of interest to be decoded. Many previous works have already addressed the SI problem from the characteristics of SI components to cancellation methods [9], providing several cancelling steps from antenna-domain to digital-domain in order to eliminate effectively various kinds of SI effects.

We focus on digital cancellation which is the last step before information decoding and concentrates on suppressing residual SI components to a very low power level by applying replica subtraction [9]. As per earlier literature, digital cancellation in OFDM systems can be executed on per-subcarrier-basis by using the interference signal directly, because the signaling format is orthogonal [10]. In contrast, applying digital cancellation in GFDM transceivers requires more sophisticated techniques, because such systems are characterized by their non-orthogonal modulation format [5]. In particular, GFDM signaling is subject to a complicated interference pattern between symbols and subcarriers at the receiver such that the digital canceller should take into account the various interference components between subchannels in order to perfectly cancel the SI.

Our main contribution is to develop a subcarrier-wise interference canceller that removes all the components of the SI based on the GFDM signal pattern. Frequency-domain cancellation is matched to multi-carrier operation by including per-subcarrier channel estimation that facilitates its implementation. However, including all SI components in cancellation requires large computational effort, which strains the system in terms of complexity. Thus, we also propose an advanced method for reducing complexity as well as analyze the trade-off between complexity and cancellation performance, which may be useful for practical system implementation.

This work was supported by the National Research Foundation of Korea(NRF) grant funded by the Korea government (NRF-2015R1A2A1A01006162).

## II. SYSTEM MODEL

### A. Full-Duplex Architecture

We consider a full-duplex system where a wireless device simultaneously transmits and receives GFDM signals in the same time slot and frequency band. The corresponding signal model is expressed in time domain as

$$r[n] = h^{(s)}[n] * x^{(s)}[n] + h^{(d)}[n] * x^{(d)}[n] + z[n] \quad (1)$$

where  $r[n]$  is the received signal at the full-duplex transceiver, and  $h^{(i)}[n]$  and  $x^{(i)}[n]$  are a time-invariant multipath channel and a transmitted signals, respectively, for  $i \in \{s, d\}$  when  $s$  and  $d$  refer to the SI and the desired signal, respectively. Term  $z[n]$  represents additive white Gaussian noise (AWGN).

The SI from the device's own transmitter is much more powerful than the desired signal, because attenuation over short distance in the loopback channel is typically very weak compared to that affecting the desired signal. Thus, self-interference cancellation (SIC) in the receiver is necessary [9]. The basic principle of SIC is to generate a replica of the transmitted signal and subtract it from the received signal.

### B. GFDM Signaling

GFDM modulation is non-orthogonal and based on block transmission with flexible resource partitioning. Each GFDM block is divided into subsymbols and subcarriers in time and frequency domain, respectively, where input signals are allocated to resource partitions. Suppose that the number of subsymbols and subcarriers in a single block are  $M$  and  $K$ , respectively. The representation of the transmitted GFDM signal in time domain before adding a CP is given by

$$\mathbf{x} = \sum_{m=0}^{M-1} \mathbf{x}_m, \quad (2a)$$

$$\mathbf{x}_m = \mathbf{G}_m \mathbf{P} \mathbf{W}_{\langle K \times K \rangle} \mathbf{a}_m = \mathbf{U}_m \mathbf{a}_m \quad (2b)$$

where  $\mathbf{x}_m$  is the  $m$ th subsymbol vector of size  $MK \times 1$  and  $\mathbf{a}_m$  is a data symbol vector at  $m$ th subsymbol time of size  $K \times 1$ . Matrix  $\mathbf{W}_{\langle K \times K \rangle}$  is a  $K \times K$  inverse DFT matrix and  $\mathbf{P}$  is an  $M$ -fold expander that consists of  $M$  identity matrices as

$$\mathbf{P} = [\mathbf{I}_{\langle K \times K \rangle}, \dots, \mathbf{I}_{\langle K \times K \rangle}]^T \quad (3)$$

where  $\mathbf{I}_{\langle K \times K \rangle}$  is a  $K \times K$  identity matrix and  $\{\cdot\}^T$  is the transpose operator. Diagonal matrix  $\mathbf{G}_m$  of size  $MK \times MK$  represents time-domain real-valued window function at  $m$ th subsymbol time. The diagonal part of  $\mathbf{G}_m$  is a circular shift of the diagonal part of  $\mathbf{G}_0$  by  $mK$  symbols. Transmission pulse response at  $m$ th subsymbol time is denoted by  $\mathbf{U}_m = \mathbf{G}_m \mathbf{P} \mathbf{W}_{\langle K \times K \rangle}$ . After adding a CP, the GFDM block (2a) is transmitted through a wireless channel.

Denote the received signal vector after removing CP by  $\hat{\mathbf{r}}$ . The frequency-domain signal vector at the receiver for subsymbol  $m'$ ,  $m' = 0, \dots, M-1$  is reconstructed by passing the received signal through GFDM demodulator

$$\mathbf{y}_{m'} = \mathbf{U}_{m'}^H \hat{\mathbf{r}} = \mathbf{W}_{\langle K \times K \rangle}^H \mathbf{P}^T \mathbf{G}_{m'} \hat{\mathbf{r}} \quad (4)$$

where  $\{\cdot\}^H$  is Hermitian operator. Finally, transmitted symbols  $\mathbf{a}_{m'}$  are decoded by applying channel equalizer to  $\mathbf{y}_{m'}$ .

An important thing to keep in mind is that the reconstructed signal inherently contains interference due to the non-orthogonal signaling. Figure 7 in [5] shows the pattern of inherent interference composed of inter-subsymbol interference (ISI), inter-carrier interference (ICI) from the same time slot's subsymbols, and ICI from the other time slot's subsymbols. Thus, creating a replica of self-interference is not straightforward but requires some complicated procedure in order to take into account the inherent interference components.

## III. SIC UNDER GFDM SIGNALING

This section provides the detailed SIC process focusing on the replica generation including the modeling of inherent interference. Especially, we will discuss the performance of SIC process in terms of its complexity and accuracy.

### A. Interference Cancellation Architecture

Figure 1 shows a block diagram of SIC architecture at the receiver. Based on (1), the model of the received subcarrier-level signal can be rewritten as

$$\begin{aligned} \mathbf{y}_{m'} &= \mathbf{U}_{m'}^H (\mathbf{H}^{(s)} \mathbf{x}^{(s)} + \mathbf{H}^{(d)} \mathbf{x}^{(d)} + \mathbf{z}) \\ &= \mathbf{y}_{m'}^{(s)} + \mathbf{y}_{m'}^{(d)} + \mathbf{U}_{m'}^H \mathbf{z}, \end{aligned} \quad (5)$$

where  $\mathbf{H}^{(i)}$  for  $i \in \{s, d\}$  refer to self-interference and desired channel matrices, respectively. When the channel delay is shorter than the CP length, the channel matrix is a circulant matrix. If the channel delay is longer than the CP length, the channel matrix is not circulant any more and the interference from the previous block occurs. When developing the proposed SIC schemes, we assume that the channel delay is shorter than the CP, but simulation results in Section IV evaluate also cases where delay spread exceeds the CP length.

Self-interference cancellation (SIC) should be applied before channel equalization of the desired signal. The reason for this is to avoid amplifying the self-interference. The cancellation process is executed per-subcarrier-basis after GFDM demodulator with the aid of replica generation process. In order to consider the ISI and ICI components of self-interference, the SIC is given by

$$\begin{aligned} \mathbf{y}_{m'}^{SIC} &= \mathbf{y}_{m'} - \sum_{m=0}^{M-1} \mathbf{C}_{m',m} \mathbf{a}_m^{(s)} \\ &= \underbrace{\left( \mathbf{y}_{m'}^{(s)} - \sum_{m=0}^{M-1} \mathbf{C}_{m',m} \mathbf{a}_m^{(s)} \right)}_{\text{SIC term}} + \mathbf{y}_{m'}^{(d)} + \mathbf{U}_{m'}^H \mathbf{z}, \end{aligned} \quad (6a)$$

where  $\mathbf{C}_{m',m}$  is the coefficient matrix for replica generation.

The main task of the replica generation process is to build the coefficient matrix based on the combination of GFDM signaling and estimated self-interference channel, and thereby to make the SIC term be zero. To reproduce the subsymbol interference of GFDM signaling, the cancellation structure contains the summation of all data symbols with its own

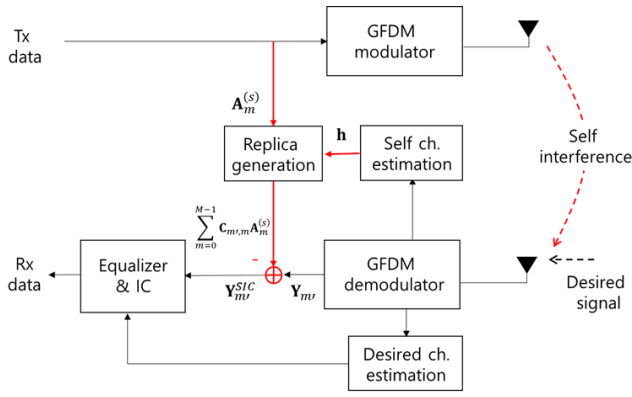


Fig. 1. GFDM-based full-duplex transceiver with self-signal cancellation.

coefficient matrix. The coefficient matrix is constructed by convolving the estimated self-interference channel with the ICI pattern. We assume that the self-interference channel is perfectly estimated per subcarrier by a frequency-domain channel estimator. Then, we can define the coefficient matrix for replica generation as

$$\mathbf{C}_{m',m} = \hat{\mathbf{G}}_{m'} \mathcal{H} \hat{\mathbf{G}}_m, \quad (7)$$

where  $\hat{\mathbf{G}}_m = \hat{\mathbf{W}}_{(K \times MK)}^H \mathbf{G}_m \hat{\mathbf{W}}_{(MK \times K)}$  is the frequency-domain filter matrix and  $\hat{\mathbf{W}}_{(MK \times K)} = \mathbf{P} \mathbf{W}_{(K \times K)}$ . Note that  $\mathcal{H}$  refers to frequency-domain self-interference channel matrix interpolated by  $M$ . The reason why the channel is interpolated is because the self-interference is passed through the channel being upsampled in frequency domain, see (2b). By using the interpolated channel, the canceller is able to duplicate the upsampled self-interference signal.

After SIC, the receiver performs the channel equalization such as least squares (LS) or minimum mean square error (MMSE), for the desired signal. An advanced receiver structure can be introduced such as successive interference cancellation that cancels the ISI and ICI of the desired signal after equalizer.

Due to non-orthogonal signaling, the SIC of GFDM system has larger computational complexity than that of orthogonal signaling like OFDM. Even though the filter response  $\hat{\mathbf{G}}_{m'}$  is deterministic, calculating full coefficient matrix requires high computational complexity. This is because the coefficient matrix should be updated whenever the self-interference channel is estimated. Thus, computational complexity should be reduced.

### B. Low-Complexity System Design

The computational complexity of the SIC architecture comes from the calculation of the coefficient matrix. As the number of subsymbols and subcarriers increases, the number of coefficients that should be calculated increases as well, which results in increased computational complexity. In order to reduce the amount of computations, we consider a method of utilizing only a subset of coefficients, referred to as the "valid set", instead of the full coefficient matrix.

The valid set of coefficients is determined based on inherent interference patterns,  $\mathbf{U}_{m'}^H \mathbf{U}_m$  for any  $m$  and  $m'$ . When  $m = m'$ , the diagonal part indicates the self-interference due to transmitted symbols  $\mathbf{a}_m$ . When  $m \neq m'$  the diagonal part indicates the ISI of self-interference pattern. The non-diagonal parts of  $\mathbf{U}_{m'}^H \mathbf{U}_m$  indicate the ICI from its own subsymbol or different subsymbols. The diagonal part of matrices cannot be ignored because of their high signal amplitude, while off-diagonal parts are small compared to the diagonal parts. Specifically, the amplitude of interference power becomes smaller the further away from the diagonal of the matrix. This observation is valid for GFDM signaling in general regardless of the channel.

Based on this observation, it is concluded that the SIC architecture can generate the replica effectively by using only the coefficients near the diagonal and ignoring the rest of the off-diagonal part. In other words, the valid set of coefficient matrix needs to contain the diagonal elements and the elements near the diagonal of matrix. Denoting  $c_{m',m}^{(i,j)}$  as the element at  $i$ th row and  $j$ th column of  $\mathbf{C}_{m',m}$ , the coefficient matrix applying the valid set is expressed as

$$\tilde{\mathbf{C}}_{m',m} = \begin{cases} c_{m',m}^{(i,j)}, & |i-j| \leq \gamma, \\ 0, & |i-j| > \gamma, \end{cases} \quad (8)$$

where  $\gamma$  is the size of valid set. The physical meaning is that the canceller reproduces only the ICI components within the range  $\gamma$  from the center subcarrier for performing SIC while the remaining weaker components are neglected.

1) *SIC Error*: Since a few coefficient elements are calculated among the coefficient matrix, the computational complexity in the receiver can be relaxed. However, as a side effect, the residual interference remains after the SIC. Although the ICI components out of range have very small amplitude, the residual interference power can be considerably high compared to the desired signal power, because the self-interference originally has high power. We define the residual interference power ratio compared to the SI power as

$$e_{SIC} = \frac{\mathbb{E} \left[ \left\| \sum_{m=0}^{M-1} (\mathbf{C}_{m',m} - \tilde{\mathbf{C}}_{m',m}) \mathbf{a}_m^{(s)} \right\|^2 \right]}{\mathbb{E} \left[ \left\| \mathbf{y}_{m'}^{(s)} \right\|^2 \right]}, \quad (9)$$

which is used to evaluate the trade-off between  $\gamma$  and SIC performance in simulation results.

2) *Computational Complexity*: The computational complexity of (7) and (6a) depends on  $\gamma$ . Equation (7) has matrix-matrix multiplications with matrix sizes of  $K \times MK$ ,  $MK \times MK$  and  $MK \times K$ . Recalling that the  $MK \times MK$  channel matrix  $\mathcal{H}$  is diagonal matrix, the number of complex-valued multiplications and additions become  $MK^3 + M^2K^2$  and  $MK^3$ , respectively. However, in the proposed low-complexity scheme, the elements in valid set need to be calculated only among  $K^2$  elements according to (8). Then, the number of elements to be calculated is reduced from  $K^2$  to  $(2\gamma + 1)K$  where  $(2\gamma + 1)$  is the number of elements in valid set. Then,

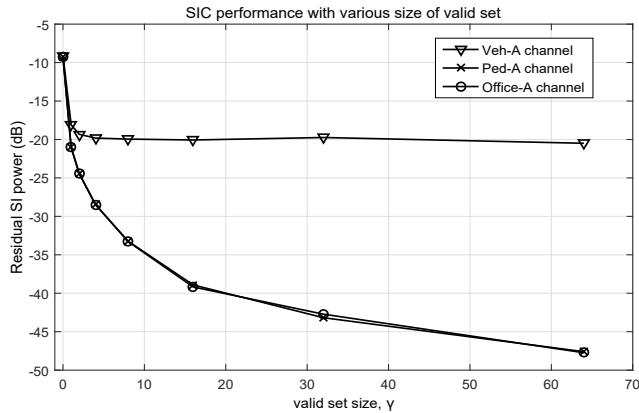


Fig. 2. Residual self-interference ratio defined as  $10 \log(e_{SIC})$  as a function of valid set size  $\gamma$  in ITU Ped-A and ITU Veh-A channels.

the number of complex-valued multiplications and additions in the proposed scheme become  $(MK^2 + M^2K)(2\gamma + 1)$  and  $MK^2(2\gamma + 1)$ , respectively.

Equation (6a) has  $M$  matrix-vector multiplications where respective sizes are  $K \times K$  and  $K \times 1$ . In the same way with the complexity evaluation of (7), the number of complex-valued multiplications and additions in the proposed scheme are reduced from  $MK^2$  and  $MK^2$  to  $MK(2\gamma + 1)$  and  $MK(2\gamma + 1)$ , respectively. Then, the total number of complex multiplications and additions in the proposed low-complexity SIC, denoted as  $\kappa_m$  and  $\kappa_a$  respectively, are

$$\begin{aligned} \kappa_m &= MK(K + M + 1)(2\gamma + 1), \\ \kappa_a &= MK(K + 1)(2\gamma + 1). \end{aligned} \quad (10)$$

We can see that the valid set size is important factor to manage system complexity. If the SI power is rather high or the first stages in SI mitigation (passive isolation and analog cancellation) do not reduce the SI power sufficiently, the proposed architecture should target to good SIC performance instead of low system complexity. Otherwise, the proposed architecture can focus on reducing the system complexity while satisfying a minimum SIC performance.

When the total system complexity is fixed, the valid set size  $\gamma$  has trade-off with the number of subcarriers  $K$ , i.e.  $\gamma \propto \frac{1}{K^2}$ , according to (10). As  $\gamma$  decreases, the number of subcarriers increases so that more data can be conveyed. However, the SIC error (9) also increases and performance is degraded. In other words, the total throughput depends on several factors affected by the valid set size. Accordingly, choosing the valid set size is important when designing practical system architecture.

#### IV. SIMULATION RESULTS AND DISCUSSION

In this section, we assess the performance of the proposed SIC architecture with respect to the residual self-interference and the corresponding bit-error rate (BER).

The performance is averaged over  $10^3$  Monte Carlo iterations with the following parameters:

- 1) The sampling frequency and the carrier frequency are set to 15.36MHz and 2GHz, as in some LTE-like system.

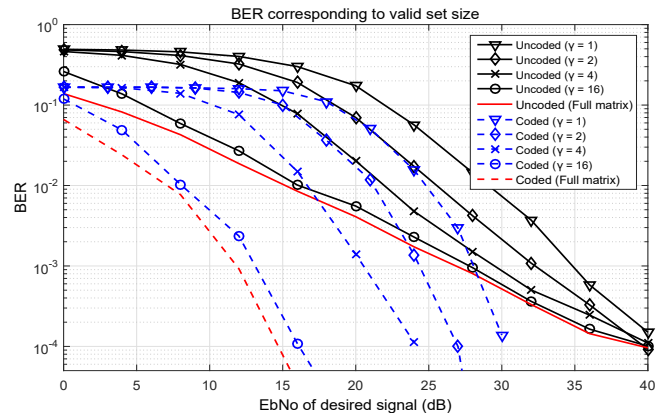


Fig. 3. BER curves corresponding to different sizes of valid set when the self-interference power is fixed to 40dB. The channel model is ITU PED-A

- 2) The number of subsymbols and subcarriers in each block is  $M = 4$  and  $K = 256$  while the subcarrier bandwidth is 15/256 MHz. The number of sequentially transmitted blocks is set to 10. The number of samples in the cyclic prefix is set to 32. The modulation type is 4-QAM.
- 3) Convolutional coding is applied with a constraint length of 7 and a coding rate of 1/3.
- 4) Pulse-shaping filter in frequency domain is the raised cosine filter with roll-off factor 0.8.
- 5) Self-interference channel models<sup>1</sup> are ITU Indoor Office A ("Office-A"), ITU Pedestrian A ("Ped-A") and ITU Vehicular A ("Veh-A") [11]. The channel model for the desired signal is ITU Ped-A.
- 6) Matched filter with successive interference cancellation is used as an equalizer for the desired signal [5].

Figure 2 shows the residual SI power ratio defined as  $10 \log e_{SIC}$  (dB) as a function of the valid set size  $\gamma$ . In Ped-A channel, the residual SI ratio is inversely proportional to  $\gamma$ . When  $\gamma$  increases more ICI components are reproduced when generating replica, which improves the performance of SIC. With  $\gamma = 64$ , the residual SI power is about -48dB in Ped-A channel. On the other hand, the residual SI power ratio in Veh-A channel saturates to -20dB irrespective of  $\gamma$ . The reason is that the delay spread of Veh-A channel is longer than the CP length giving rise to inter-block interference (IBI). Since the SIC architecture does not include IBI cancellation, the IBI components of SI remains, which degrades the SIC performance.

Figure 3 shows coded and uncoded BER at the full-duplex receiver when applying the proposed SIC architecture with different  $\gamma$ . The x-axis indicates the energy per bit to noise power spectral density ratio (EbNo) of the desired signal. The self-interference power is fixed to 40dB and the channel

<sup>1</sup>With passive cancellation, the self-interference channel becomes more frequency-selective since the passive suppression reduces the direct line-of-sight path for self-interference. For this reason, we adopt ITU channel models as the frequency selective channels. The path loss according to the distance is considered as the received signal power.

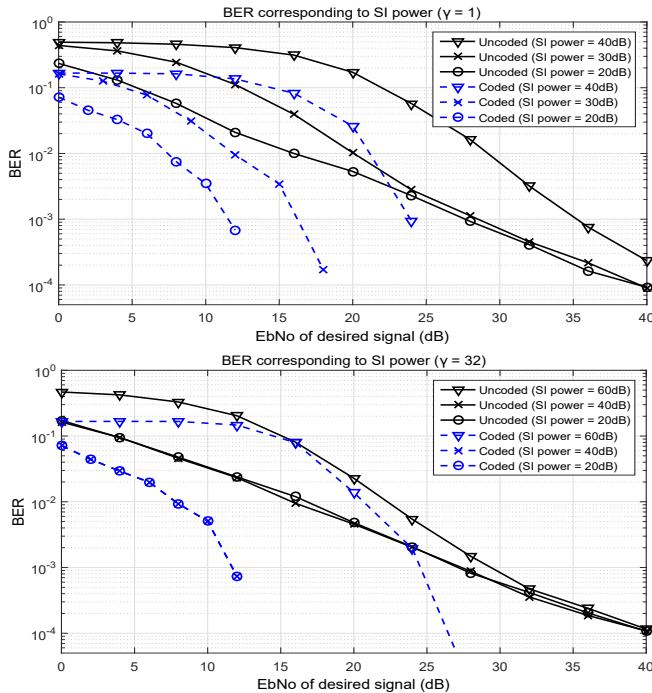


Fig. 4. BER curves corresponding to different powers of self-interference when the valid set size is 1 (upper figure) and 32 (lower figure). The channel model follows ITU PED-A model.

follows ITU Ped-A model. As the valid set size increases, the uncoded BER performance becomes better and gets close to the perfect SIC case that uses the full coefficient matrix. The behavior of coded BER corresponding to valid set size is similar to that of uncoded BER. Note that the BER curves of  $\gamma = 16$  case almost reaches that of the perfect case. This is because when  $\gamma = 16$  SI power is reduced by about 40dB as shown in Fig. 2. Accordingly, for the given environment, the SIC architecture with  $\gamma = 16$  is the best choice to improve system performance with reduced complexity.

Figure 4 depicts BER performance with different levels of self-interference power in the ITU-Ped A channel. The upper and the lower figure correspond to  $\gamma = 1$  and  $\gamma = 32$ , respectively. For  $\gamma = 1$  the performance gets close to the bound when the SI power is around 20dB, because according to Fig. 2 self-interference power is reduced by -18dB when  $\gamma = 1$ . However,  $\gamma = 1$  is clearly insufficient when SI power becomes larger. In case SI power is 40 dB,  $\gamma = 32$  is a proper choice to reduce complexity without degrading performance.

Based on the coded BER results, we provide throughput curves when the complexity of the receiver is constrained. For given complexity, both the number of subcarriers and coded BER value depend on  $\gamma$ . Hence, we can express the throughput as  $\hat{K}(\gamma)[1 - BER_{coded}(\gamma)]$  where  $\hat{K}$  is the number of subcarriers for given complexity. Figure 5 shows the throughput curves when  $\hat{K}(1) = K = 256$ . Throughput is inversely proportional to  $\gamma$ , which implies that the effect of  $\hat{K}$  on throughput is more dominant than the effect of SIC performance when computational complexity is limited.

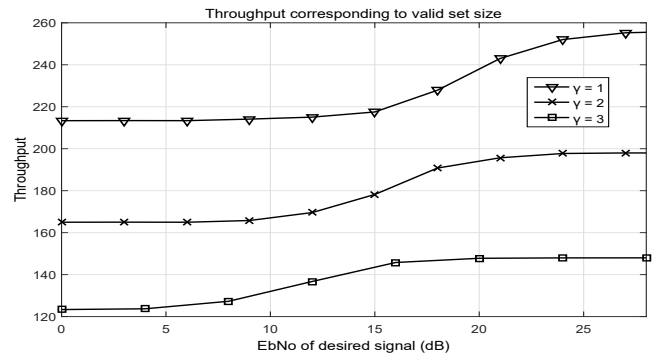


Fig. 5. Throughput corresponding to different sizes of valid set when the total complexity is fixed

## V. CONCLUSION

We investigated an architecture for self-interference cancellation under generalized frequency-division multiplexing. Due to non-orthogonal signaling, it is necessary to regenerate and remove inter-symbol and inter-carrier interference in the transmitted signal, which increases computational complexity. Instead of incorporating all interference components, we proposed the method to cancel their valid subset only. By selecting a proper size of valid set according to self-interference power, it is possible to improve the system performance and reduce the computational complexity simultaneously.

## REFERENCES

- [1] B. Farhang-Boroujeny, "OFDM versus filter bank multicarrier," *IEEE Signal Processing Magazine*, vol. 28, no. 3, pp. 92–112, May 2011.
- [2] G. Wunder et al., "5GNOW: Intermediate frame structure and transceiver concepts," in *Proc. Globecom Workshops*, Dec. 2014, pp. 565–570.
- [3] N. Michailow, M. Matthe, I. Gaspar, A. Caldevilla, L. Mendes, A. Festag, and G. Fettweis, "Generalized Frequency Division Multiplexing for 5th Generation Cellular Networks," *IEEE Transactions on Communications*, vol. 62, no. 9, pp. 3045–3061, Sep. 2014.
- [4] I. Gaspar, L. Mendes, M. Matthe, N. Michailow, A. Festag, and G. Fettweis, "LTE-compatible 5G PHY based on generalized frequency division multiplexing," in *2014 11th International Symposium on Wireless Communications Systems*, Aug. 2014, pp. 209–213.
- [5] B. M. Alves, L. L. Mendes, D. A. Guimaraes, and I. S. Gaspar, "Performance of GFDM over Frequency-Selective Channels," in *Proc. Int. Workshop Telecommun.*, May 2013.
- [6] F. Kaltenberger, R. Knopp, M. Danneberg, and A. Festag, "Experimental analysis and simulative validation of dynamic spectrum access for coexistence of 4G and future 5G systems," in *2015 European Conference on Networks and Communications*, Jun. 2015, pp. 497–501.
- [7] S. Hong, J. Brand, J. Choi, M. Jain, J. Mehlman, S. Katti, and P. Levis, "Applications of self-interference cancellation in 5G and beyond," *IEEE Communications Magazine*, vol. 52, no. 2, pp. 114–121, Feb. 2014.
- [8] D. Kim, H. Lee, and D. Hong, "A Survey of In-Band Full-Duplex Transmission: From the Perspective of PHY and MAC Layers," *IEEE Communications Surveys Tutorials*, vol. 17, no. 4, pp. 2017–2046, Oct.–Dec. 2015.
- [9] D. Bharadia, E. McMillin, and S. Katti, "Full duplex radios," in *ACM SIGCOMM Computer Communication Review*, vol. 43, no. 4, 2013, pp. 375–386.
- [10] D. Korpi, L. Anttila, V. Syrjala, and M. Valkama, "Widely Linear Digital Self-Interference Cancellation in Direct-Conversion Full-Duplex Transceiver," *IEEE Journal on Selected Areas in Communications*, vol. 32, no. 9, pp. 1674–1687, Sep. 2014.
- [11] Recommendation ITU-R M. 1225: Guidelines for evaluation of radio transmission technologies for IMT-2000, 1997.